Supporting Information

Red-Shifted Delayed Fluorescence at the Expense of Photoluminescence Quantum Efficiency – An Intramolecular Charge-Transfer Molecule Based on a Benzo[1,2-*b*:4,5-*b*']dithiophene-4,8-dione Acceptor

Stephanie Montanaro,[a] Alexander J. Gillett,[b] Sascha Feldmann,[b] Emrys W. Evans,[b] Felix Plasser,[a] Richard H. Friend,[b]* and Iain A. Wright[a]*

[a] *Department of Chemistry, Loughborough University, Loughborough, Leicestershire, LE11 3TU, U.K.*

[b] *Optoelectronics Group, Cavendish Laboratory, University of Cambridge, Cambridge, CB3 0HE, U.K.*

General Experimental:

All reactants and reagents were purchased from commercial suppliers and used without further purification unless otherwise stated. Column chromatography was carried out using silica gel 60, 40−60 μm mesh (Fluorochem). Analytical thin-layer chromatography was performed on precoated aluminum silica gel 60 F254 plates (Merck), which were approximately 2 cm × 6 cm in size, and visualized using ultraviolet light (254/365 nm).

NMR spectra were recorded on Jeol ECS 400 MHz and Jeol ECZ 500 MHz spectrometers. Chemical shifts are reported in ppm downfield of tetramethylsilane (TMS) using TMS or the residual solvent as an internal reference. NMR spectra were processed using MestReNova. Multiplicities are reported as singlet (s), doublet (d), triplet (t), and multiplet (m). Melting points were determined in open-ended capillaries using a Stuart Scientific SMP10 melting point apparatus at a ramping rate of 1 °C/min. They are recorded to the nearest 1 °C and are uncorrected. IR spectra were collected on a Thermo Scientific Nicolet FTIR spectrometer. Atmospheric solids analysis probe (ASAP) mass spectra were recorded on a Waters LCT Premier XE spectrometer. The sample was introduced as a solid, applied directly to a glass probe tip. Elemental analyses were obtained on an Exeter Analytical CE440 Elemental analyser.

Thermogravimetric analysis were performed using a TA SDT Q600 instrument. Two alumina crucibles with a small amount of sample (5-10 mg) and an as close to equal (± 0.01 mg) amount of alumina reference powder were used for the analysis. Temperature was increased at a rate of 5 °C/min from 25 °C to 800 °C. Data obtained was analysed using TA Instruments Universal Analysis 2000 (Version 4.5A, Build 4.5.0.5) software.

Cyclic voltammetry was recorded using a Princeton Applied Research VersaSTAT 3. A glassy carbon disk, Pt wire, and Ag/Ag^+ ($AgNO_3$ in acetonitrile) were used as the working, counter, and reference electrodes, respectively. Measurements were corrected to the ferrocene/ferrocenium redox couple as an internal standard. 1,2-Dichlorobenzene was used as the solvent with an analyte molarity of ca. 10^{-5} M in the presence of 10^{-1} M (*n*-Bu_4N) (PF_6) as a supporting electrolyte. Solutions were degassed with Ar and experiments run under a blanket of Ar.

A ground-state structure optimisation using density functional theory (DFT) was performed with ORCA v4.0.1.2[1] using the B3LYP functional and 6-31G* basis set[2,3] and modelled in toluene as solvent. The orbitals plotted in Fig. 1 were computed at the same level of theory. Vertical excitation energies (Table S1) were computed at the ωPBEh/cc-pVDZ level[4,5] using a value of ω=0.1 a.u. within Q-Chem 5.1.[6] A non-equilibrium formalism was used to model the effect of toluene solvation.[7]

Synthetic Methods

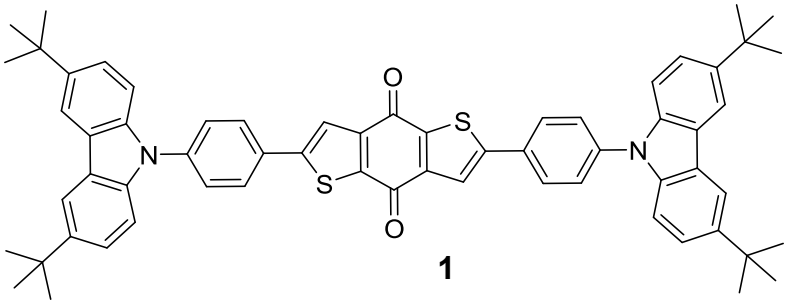

1

An oven dried two neck flask fitted with a condenser was placed under a N_2 atmosphere. Dibromide **3** (69 mg, 0.18 mmol) and K_2CO_3 (75 mg, 0.54 mmol, 3.0 eq.) were added to the flask followed by tetrahydrofuran (15 mL) and water (5 mL). The mixture was thoroughly degassed by bubbling with N_2 for 45 min. Broronic acid **4** (164 mg, 0.40 mmol, 2.2 eq.) was added and the mixture degassed for a further 5 min. $Pd(PPh_3)_4$ (3 mg, 3 μmol, 2 mol%) was added and the mixture heated to 55 °C for 24 h. Water (25 mL) was added and the crude product was isolated as a purple solid by filtration. The solid obtained was then dissolved in boiling *N*,*N*-dimethylformamide (*ca.* 50 mL), and passed through a plug of silica (⌀ 30 mm × 5 mm) eluting with further hot *N*,*N*-dimethylformamide (total volume *ca.* 150 mL). Upon cooling the filtrate a precipitate formed which was isolated via filtration to obtain **1** as a purple solid (110 mg, 66%). mp. > 300 °C

N.B. Addition of a few drops of CS_2 to the NMR sample was required to inhibit aggregation and obtain well-resolved NMR spectra.

^{1}H NMR (400 MHz, Chloroform-*d*, ppm) δ = 8.15 (d, *J* = 1.4 Hz, 4H), 7.94 (s, 2H), 7.94 (d, *J* = 8.6 Hz, 4H), 7.70 (d, *J* = 8.6 Hz, 4H), 7.50 (dd, *J* = 8.7, 1.9 Hz, 4H), 7.44 (d, *J* = 8.7 Hz, 4H), 1.48 (s, 36H)

^{13}C NMR (126 MHz, Chloroform-*d*, ppm) δ = 173.8, 152.1, 143.9, 143.2, 142.5, 139.7, 138.6, 130.5, 127.8, 126.9, 123.9, 123.8, 122.1, 116.5, 109.2, 34.6, 32.0

IR (ν_{max}/cm^{-1}) 2953, 2865, 1653 (C=O, s), 1601, 1530, 1470, 1434, 1264, 1179, 838, 821

MS (ASAP$^+$): m/z = 927.4 [M+H$^+$]

HRMS (ASAP$^+$): m/z = calculated for $C_{62}H_{59}N_2O_2S_2$ [M+H$^+$]: 927.4012; found: 927.4025

Elemental analysis: Calculated for $C_{62}H_{58}N_2O_2S_2$: C, 80.31; H, 6.30; N 3.02. Found C, 80.12; H, 6.22; N, 3.13

Copies of NMR Spectra of Compound 1

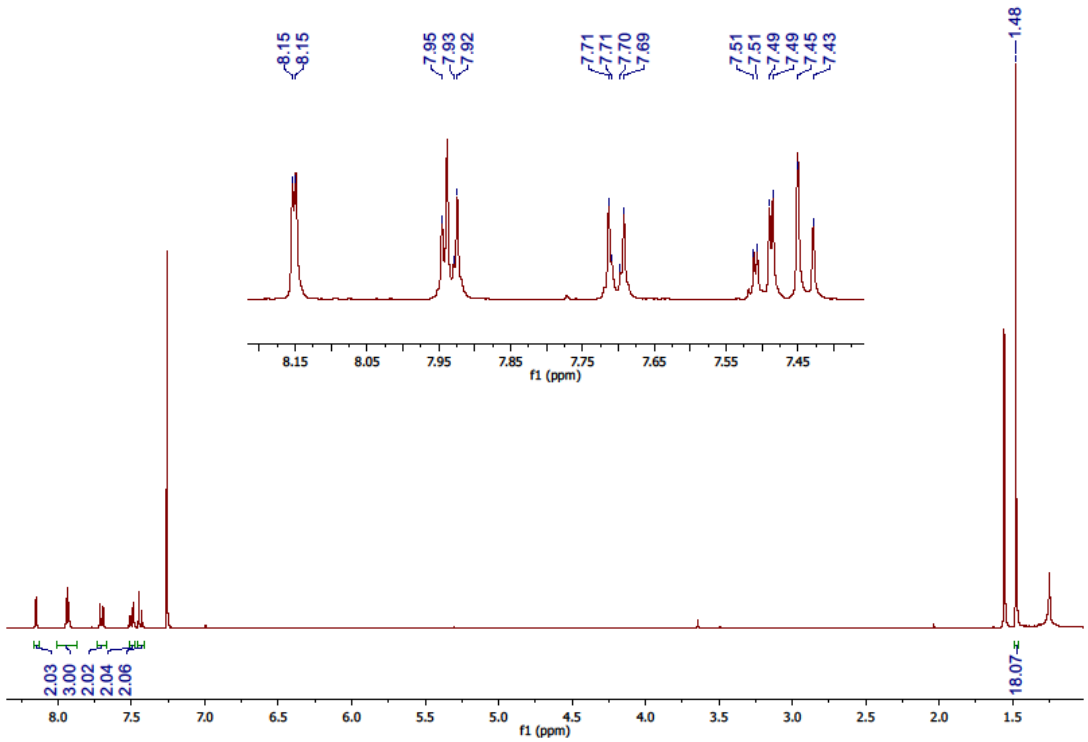

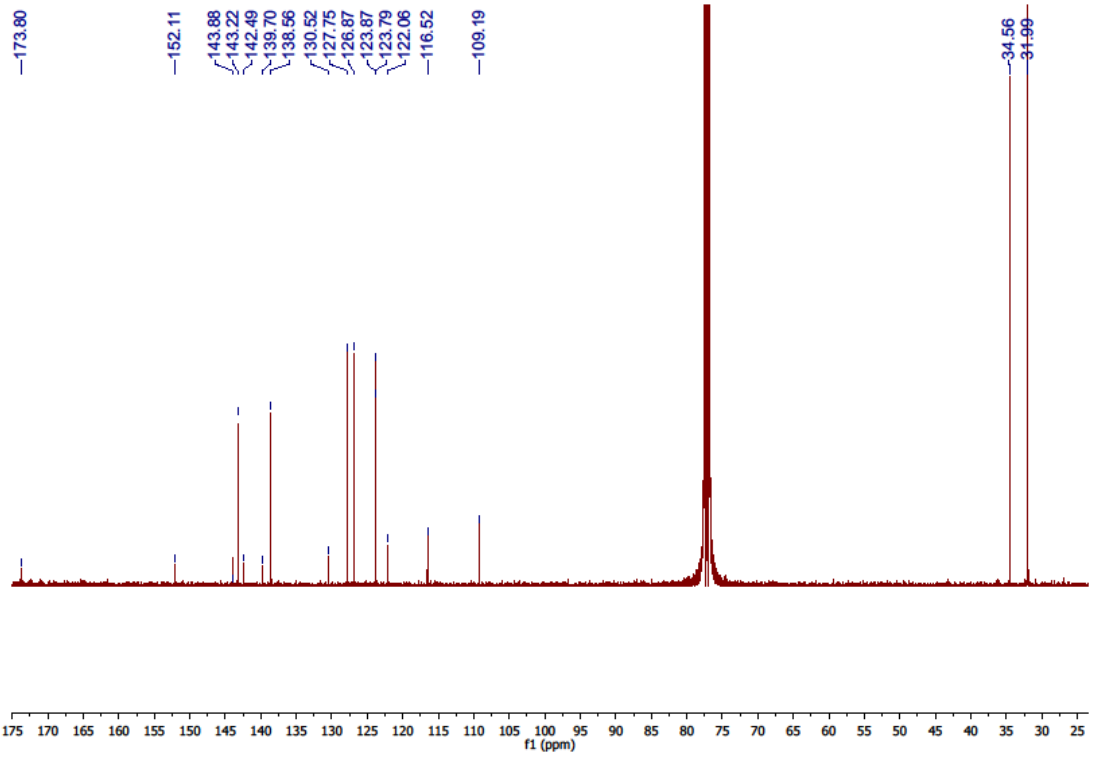

Thermal Gravimetric Analysis

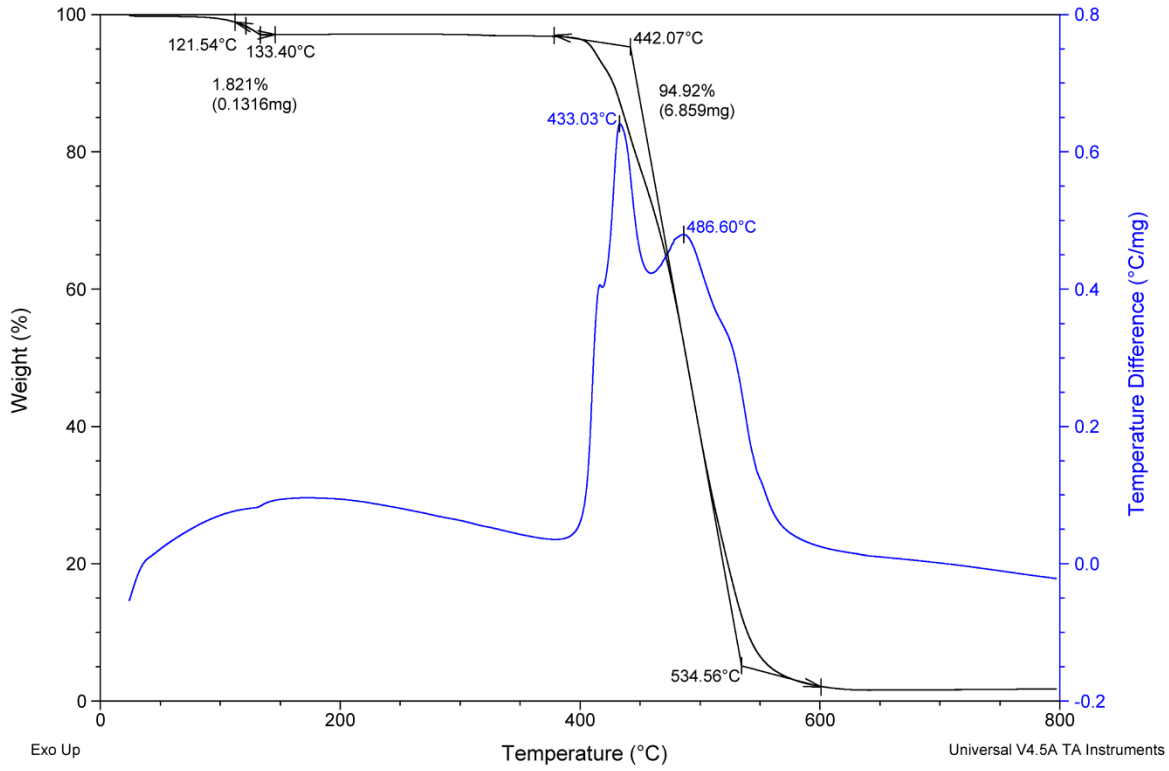

Figure S1 Thermal gravimetric analysis (black line) of compound **1**.

Photophysics

Experimental Details

Sample fabrication

Solutions of **1** and polystyrene were created in toluene with a total concentration of 100 mg/mL, consisting of 2 wt % **1**. These solutions were then drop cast onto substrates warmed to 80^{o}C. All films were deposited onto spectrosil fused silica substrates that were first cleaned by sonicating in acetone and isopropanol for 10 minutes each. Films for optical studies were encapsulated under glass in an inert N_2 atmosphere prior to use.

Transient absorption spectroscopy

The TA experiments were performed using a commercially available Ti:sapphire amplifier (Spectra Physics Solstice Ace). The amplifier operates at 1 kHz and generates 100 fs pulses centered at 800 nm. For the ultrafast measurements, the 400 nm pump is generated by frequency doubling the 800 nm output of the Ti:sapphire in a beta barium borate (BBO) crystal. The residual 800 nm was removed from the pulse using a BG39 coloured glass filter. For the long-time TA, a 1 ns duration pump pulse is provided by the third harmonic (355 nm) of an electronically triggered Q-switched Nd:YVO_4 laser (Advanced Optical Technologies Ltd AOT-YVO-25QSPX). For both the ultrafast and long-time TA, the probe pulses used in our experiments were provided by NOPAs operating in the visible (510 – 780 nm) and NIR (830 -1025 nm) regions. The transmitted probe pulses were then collected with a silicon dual-line array detector (Hamamatsu S8381-1024Q) driven and read out by a custom-built board from Stresing Entwicklungsbüro.

Ultrafast (fs-ps) transient grating photoluminescence measurements

A Ti:Sapphire amplifier system (Spectra Physics Solstice Ace) operating at 1 kHz generating 100 fs pulses was split into the pump and probe beam arms. The pump beam was generated by second harmonic generation (SHG) in a BBO crystal and focused onto the sample. The photoluminescence generated is collimated using a silver off-axis parabolic mirror and focused onto the gate medium. About 80 μJ/pulse of the 800 nm laser output is used for the gate beams, which is first raised 25 mm above the plane of the PL to produce a boxcar geometry and split into a pair of gate beams using a 50/50 beam splitter. The gate beams are focused onto the gate medium (fused silica), crossing at an angle of ~5° and overlapping with the focused PL. The two gate beams interfere and create a transient grating in the gate medium due to a modulation of the refractive index via the optical Kerr effect. Temporal overlap between the two gate beams is achieved via a manual delay stage. The PL is then deflected on the transient grating causing a spatial separation of the gated signal from the PL background. Two lenses collimate and focus the gated signal onto the spectrometer entrance (Princeton Instruments SP 2150) after long- and short-pass filters remove scattered pump and gate light, respectively. Gated PL spectra are measured using an intensified CCD camera (Princeton Instruments, PIMAX4). The (~10 ns) electronic shutter of the intensified CCD camera was used to further suppress long-lived PL background. PL spectra at each gate time

delay are acquired from ~10000 laser shots. The time delay between pump and gate beams is controlled via a motorized optical delay line on the excitation beam path and a LabVIEW data acquisition program.

Time-resolved (ns-µs) photoluminescence

Time-resolved PL spectra were recorded using an electrically-gated intensified CCD camera (Andor iStar DH740 CCI-010) connected to a calibrated grating spectrometer (Andor SR303i). Sample excitation with a 400 nm pump pulse was provided by frequency doubling a small portion of the Ti:sapphire 800 nm output in a BBO crystal. The residual 800 nm was removed from the pulse using a BG39 coloured glass filter. Temporal evolution of the photoluminescence emission was obtained by stepping the ICCD gate delay with respect to the excitation pulse.

Steady-state absorption

Steady-state absorption spectra were measured using an HP 8453 spectrometer.

Steady-state photoluminescence and photoluminescence quantum efficiency

The PLQE was determined using method previously described by De Mello *et al.*.[8] The steady-state PL was measured simultaneously. Samples were placed in an integrating sphere and were photoexcited using 405 and 520 nm continuous-wave lasers. The laser and the emission signals were measured and quantified using a calibrated Andor iDus DU420A BVF Si detector.

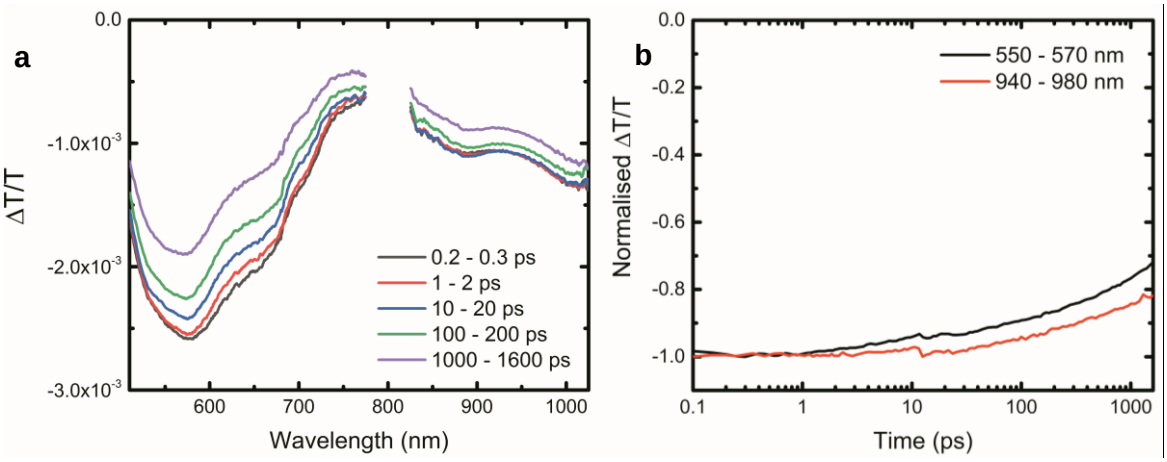

Figure S2 a Short time TA spectrum of a film of **1** doped at 2 wt% in polystyrene, taken at different time points. The film was excited at λ_{ex} = 400 nm, with a fluence of 88 μJ/cm^2. **b** The normalised kinetics taken from the wavelength regions of 550 – 570 nm and 940 – 980 nm.

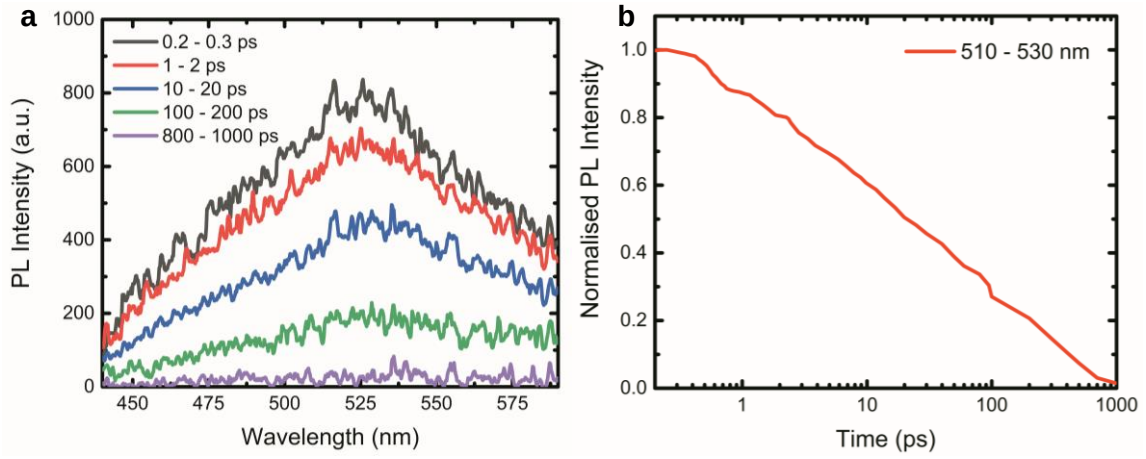

Figure S3 a PL spectrum of a film of **1** doped at 2 wt% in polystyrene, taken at different time points. The film was excited at λ_{ex} = 400 nm, with a fluence of 306 μJ/cm^2. **b** The normalised PL kinetics taken from the wavelength regions of 510 – 530 nm.

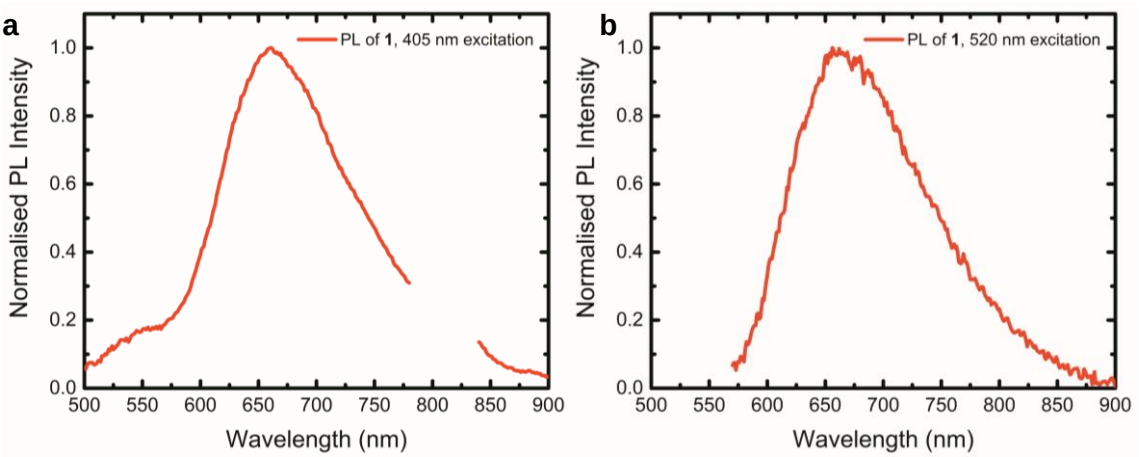

Figure S4 Steady-state PL of a film of **1** doped at 2 wt% in polystyrene the film was excited at **a** λ_{ex} = 405 nm and **b** λ_{ex} = 520 nm. A new PL band between 500 – 560 nm is visible which is not present when the sample is excited at 520 nm.

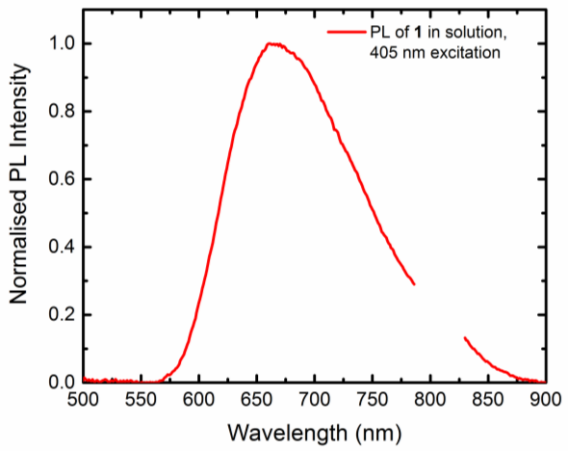

Figure S5 Steady-state PL of a solution of **1** dissolved in toluene at 0.5 mg/ml. The solution was excited at λ_{ex} = 405 nm.

Rate Constant Equations

$$k_r^S = \Phi k_p \quad \text{(S1)}$$

$$k_{ISC} = (1 - \Phi_F)k_p \quad \text{(S2)}$$

$$k_{RISC} = \frac{k_p k_d}{k_{ISC}} \frac{\Phi_d}{\Phi_F} \quad \text{(S3)}$$

$$k_{nr}^T = k_d - \Phi_F k_{RISC} \quad \text{(S4)}$$

Time-Dependent DFT

Table S1 Vertical absorption energies ($\Delta E_{abs,\ vert}$, eV) and wavelengths ($\lambda_{abs,\ vert,}$ nm), oscillator strengths (*f*), type assignments, and acceptor orbital for the lowest 10 singlet and 15 triplet excited states of compound **1** computed at the ωPBEh/cc-pVDZ level of theory.

	$\Delta E_{abs,\ vert}$	$\lambda_{abs,\ vert}$	*f*	Type	Acc. Orb.
T_1	1.95	635		ππ* (BDT)	LUMO
T_2	2.24	553		ππ* (BDT)	LUMO
S_1	2.49	498	0.00	ππ* (BDT)	LUMO
T_3	2.54	489		nπ*	LUMO
T_4	2.66	466		nπ*	LUMO
S_2	2.72	456	0.62	ππ* (Carb→BDT)	LUMO
T_5	2.93	424		ππ* (Carb→BDT)	LUMO
T_6	2.98	417		ππ* (Carb→BDT)	LUMO
S_3	2.98	415	0.01	nπ*	LUMO
T_7	3.04	408		ππ* (BDT)	LUMO
T_8	3.10	400		ππ* (Carb→BDT)	LUMO+1
S_4	3.10	400	0.00	nπ*	LUMO
S_5	3.14	395	0.01	ππ* (Carb→BDT)	LUMO
T_9	3.20	388		ππ* (Carb→BDT)	LUMO+1
T_{10}	3.22	385		ππ* (BDT)	LUMO
T_{11}	3.32	374		ππ* (Carb→Carb)	
T_{12}	3.36	369		ππ* (Carb→Carb)	
T_{13}	3.39	366		ππ* (Carb→Carb)	
T_{14}	3.41	364		ππ* (Carb→Carb)	
S_6	3.43	361	0.00	ππ* (Carb→BDT)	LUMO
T_{15}	3.46	359		ππ* (Carb→BDT)	LUMO
S_7	3.50	355	0.02	ππ* (BDT)	LUMO
S_8	3.52	352	0.00	ππ* (Carb→BDT)	LUMO
S_9	3.61	343	1.87	ππ* (Carb→BDT)	LUMO+1
S_{10}	3.72	333	0.03	ππ* (Carb→BDT)	LUMO+1

References

1 F. Neese, *Wiley Interdiscip. Rev. Comput. Mol. Sci.*, 2012, **2**, 73–78.

2 W. J. Hehre, K. Ditchfield and J. A. Pople, *J. Chem. Phys.*, 1972, **56**, 2257–2261.

3 M. M. Francl, W. J. Pietro, W. J. Hehre, J. S. Binkley, M. S. Gordon, D. J. DeFrees and J. A. Pople, *J. Chem. Phys.*, 1982, **77**, 3654–3665.

4 T. H. Dunning, *J. Chem. Phys.*, 1989, **90**, 1007–1023.

5 M. A. Rohrdanz, K. M. Martins and J. M. Herbert, *J. Chem. Phys.*, 2009, **130**, 054112.

6 Y. Shao, Z. Gan, E. Epifanovsky, A. T. B. Gilbert, M. Wormit, J. Kussmann, A. W. Lange, A. Behn, J. Deng, X. Feng, D. Ghosh, M. Goldey, P. R. Horn, L. D. Jacobson, I. Kaliman, R. Z. Khaliullin, T. Kuš, A. Landau, J. Liu, E. I. Proynov, Y. M. Rhee, R. M. Richard, M. A. Rohrdanz, R. P. Steele, E. J. Sundstrom, H. L. Woodcock, P. M. Zimmerman, D. Zuev, B. Albrecht, E. Alguire, B. Austin, G. J. O. Beran, Y. A. Bernard, E. Berquist, K. Brandhorst, K. B. Bravaya, S. T. Brown, D. Casanova, C. M. Chang, Y. Chen, S. H. Chien, K. D. Closser, D. L. Crittenden, M. Diedenhofen, R. A. Distasio, H. Do, A. D. Dutoi, R. G. Edgar, S. Fatehi, L. Fusti-Molnar, A. Ghysels, A. Golubeva-Zadorozhnaya, J. Gomes, M. W. D. Hanson-Heine, P. H. P. Harbach, A. W. Hauser, E. G. Hohenstein, Z. C. Holden, T. C. Jagau, H. Ji, B. Kaduk, K. Khistyaev, J. Kim, J. Kim, R. A. King, P. Klunzinger, D. Kosenkov, T. Kowalczyk, C. M. Krauter, K. U. Lao, A. D. Laurent, K. V. Lawler, S. V. Levchenko, C. Y. Lin, F. Liu, E. Livshits, R. C. Lochan, A. Luenser, P. Manohar, S. F. Manzer, S. P. Mao, N. Mardirossian, A. V. Marenich, S. A. Maurer, N. J. Mayhall, E. Neuscamman, C. M. Oana, R. Olivares-Amaya, D. P. Oneill, J. A. Parkhill, T. M. Perrine, R. Peverati, A. Prociuk, D. R. Rehn, E. Rosta, N. J. Russ, S. M. Sharada, S. Sharma, D. W. Small, A. Sodt, T. Stein, D. Stück, Y. C. Su, A. J. W. Thom, T. Tsuchimochi, V. Vanovschi, L. Vogt, O. Vydrov, T. Wang, M. A. Watson, J. Wenzel, A. White, C. F. Williams, J. Yang, S. Yeganeh, S. R. Yost, Z. Q. You, I. Y. Zhang, X. Zhang, Y. Zhao, B. R. Brooks, G. K. L. Chan, D. M. Chipman, C. J. Cramer, W. A. Goddard, M. S. Gordon, W. J. Hehre, A. Klamt, H. F. Schaefer, M. W. Schmidt, C. D. Sherrill, D. G. Truhlar, A. Warshel, X. Xu, A. Aspuru-Guzik, R. Baer, A. T. Bell, N. A. Besley, J. Da Chai, A. Dreuw, B. D. Dunietz, T. R. Furlani, S. R. Gwaltney, C. P. Hsu, Y. Jung, J. Kong, D.

S. Lambrecht, W. Liang, C. Ochsenfeld, V. A. Rassolov, L. V. Slipchenko, J. E. Subotnik, T. Van Voorhis, J. M. Herbert, A. I. Krylov, P. M. W. Gill and M. Head-Gordon, *Mol. Phys.*, 2015, **113**, 184–215.

7 J. M. Mewes, Z. Q. You, M. Wormit, T. Kriesche, J. M. Herbert and A. Dreuw, *J. Phys. Chem. A*, 2015, **119**, 5446–5464.

8 J. C. de Mello, H. F. Wittmann and R. H. Friend, *Adv. Mater.*, 1997, **9**, 230–232.